Research Square

Preprints are preliminary reports that have not undergone peer review. They should not be considered conclusive, used to inform clinical practice, or referenced by the media as validated information.

miR-874 ameliorates retinopathy in diabetic rats by NF-κB signaling pathway

Rui Li
Xiaogan Hospital Affiliated to Wuhan University of Science and Technology
Huimin Yuan
Xiaogan Hospital Affiliated to Wuhan University of Science and Technology
Tao Zhao
Xiaogan Hospital Affiliated to Wuhan University of Science and Technology
Yimin Yan
Xiaogan Hospital Affiliated to Wuhan University of Science and Technology
Zhaochen Liu
Xiaogan Hospital Affiliated to Wuhan University of Science and Technology
Jiayu Cai
Xiaogan Hospital Affiliated to Wuhan University of Science and Technology
Chunli Qiu
Xiaogan Hospital Affiliated to Wuhan University of Science and Technology
Chuanjing Li (lichuanjing35gh@163.com)
Xiaogan Hospital Affiliated to Wuhan University of Science and Technology https://orcid.org/0000-0002-4773-3426

Research article

Keywords: diabetic retinopathy, Rela (p65), rat, miR-874, NF-κB

Posted Date: June 2nd, 2020

DOI: https://doi.org/10.21203/rs.2.14609/v4

License: This work is licensed under a Creative Commons Attribution 4.0 International License. Read Full License

---

Version of Record: A version of this preprint was published at Advances in Clinical and Experimental Medicine on April 29th, 2021. See the published version at https://doi.org/10.17219/acem/130602.

Abstract

Background: miRNAs participate in the development and progression of diabetic retinopathy (DR). High expression of NF-κB signaling pathway boosts the progression of retinopathy in diabetes rats. We found a site where miR-874 bound to the NF-κB p65 by a bioinformatics website. Therefore, we speculated that miR-874 might improve retinopathy in diabetic rats by inhibiting the NF-κB signaling pathway.

Methods: Ten healthy rats were taken as the control group. Sixty streptozotocin (60 mg/kg)-induced diabetes model rats were randomly divided into the model group (injection of normal saline), NC (negative control) agomir group (injection of NC mimic), miR-874 agomir group (injection of miR-874 mimic), miR-874 anti-agomir group (injection of miR-874 inhibitor), EVP4593 group (injection of NF-κB signaling pathway antagonist EVP4593), and miR-874 anti-agomir + EVP4593 group (injection of miR-874 inhibitor and EVP4593). All injection was via caudal vein.

Results: miR-874 could target the degradation of p65. Compared with the control group, model rats had reduced miR-874 expression, increased VEGF and Ang2 protein expressions, lowered end-diastolic velocity and peak systolic velocity of central retinal artery (CRA) and blood velocity of central retinal vein and CRA, heightened plasma viscosity, blood viscosity and erythrocyte sedimentation rate at all shear rates, decreased capillary pericytes, increased vascular endothelial cells, and ascended p65 expression in the retina (all $P < 0.05$). It showed that pathological changes appeared in the retina of diabetes rats. These indexes would be improved in diabetes rats injected with miR-874 mimic or EVP4593, but deteriorated in those injected with miR-874 inhibitor (all $P < 0.05$). EVP4593 could alleviate the aggravation of retinopathy that was caused by miR-874 inhibition in diabetes rats.

Conclusions: miR-874 mediates the NF-κB signaling pathway by targeting the degradation of p65 to further improve the retina of diabetes rats, showing the improvement effect of miR-874 on diabetic retinopathy in rats.

Background

The incidence of China diabetes is high in China and there are over 100 million patients with diabetes. Diabetes can induce retinopathy, which is an important reason why diabetes can cause visual disturbance and even blindness [1-3]. Diabetic retinopathy (DR) is a kind of microvascular complication, and it is triggered by the leakage of retinal capillary wall caused by the hyperglycemia of diabetic patients. However, its pathogenesis is complicated and not fully understood. Previous studies suggested that a series of pathophysiological changes happened on the retina under the stimulation of persistent hyperglycemia, resulting in retinopathy [4-8].

Diabetes rats had abnormal activation of NF-κB signaling pathway, which augments the generation of reactive oxygen species and further leads to the occurrence of microaneurysms, retinal neovascularization and vitreous hemorrhage, boosting the progression of retinopathy in diabetes rats [9-11].

Encoded by endogenous gene, microRNA (miRNA) is a non-coding single-stranded RNA molecule, which has the features of high conservation, time sequence and tissue specificity [12, 13]. miRNAs can regulate the protein expression a specific target gene by interacting with the 3'UTR region of its mRNA via sequence-specific mode. Recent studies have revealed that miRNAs participate in the development and progression of DR and are involved in multiple pathogenesis of DR [14-16]. We found a site where miR-874 bound to the NF-κB p65 by the bioinformatics website, and the down-regulation of miR-874 expression in rats with myocardial ischemia reperfusion injury exerted an inhibitory effect on inflammation and injury [17, 18]. However, no study had reported the relationship between miR-874 and DR, and it was unknown whether miR-874 regulated DR and whether NF-κB p65 acted as a downstream regulatory element for miR-874 in DR.

Therefore, in our study, DR rat models were established and treated with genetic intervention to explore the effect of miR-874 on DR rats and the regulatory relationship between miR-874 and NF-κB signaling pathway. The results were conducive to further understand the pathogenesis of DR and provided a theoretical foundation for taking miR-874 as a potential target for new drugs in the treatment of DR.

Methods

Cell culture

HEK293T cells from the American Type Culture Collection were used in the dual-luciferase reporter assay. HEK293T cells were cultured in the DMEM containing 10% fetal bovine serum by routine methods. Cells were passaged and cultured in fresh complete medium every three days.

Dual-luciferase reporter system assay

The bioinformatics prediction website (www.targetscan.org) predicted that there was a binding site between miR-874 and Rela (p65), which was then verified by dual-luciferase reporter system assay. The reporter plasmids containing target gene Rela (pmirGLO-Rela wt) and the mutant in the target gene (pmirGLO-Rela mut) were constructed, respectively. These two reporter plasmids were co-transfected with NC mimic or miR-874 mimic into HEK 293T cells, respectively. After transfection for 24 h, the dual-luciferase reporter assay was performed according to the instruction of dual-luciferase reporter assay kit (Promega). Relative luciferase activity = firefly luciferase activity / renilla luciferase activity.

Establishment of diabetes rat models

Streptozotocin (STZ) was used to induce diabetes rat models. Ninety male Sprague-Dawley rats (200-250 g, 8 weeks old, from the Laboratory Animal Center of Chongqing Medical University, China) were fed with standard food and water in the laboratory under specific pathogen free condition. Ten rats were randomly

selected as the control group, and the rest were used to construct models. Citrate buffer solutions (pH 4.5) were used to prepare fresh STZ solutions. Single intraperitoneal injection of 60 mg/kg STZ solutions was performed in rats to induce diabetes. One week later, the rat with fasting blood glucose above 250 mg/dl was considered to be a successful model [19]. There were 71 successfully modeled rats. The protocol and procedures employed were ethically reviewed and approved by the Ethics Committee of Xiaogan Central Hospital (2017010) and in compliance with the statement of Association for Research in Vision and Ophthalmology for the care and use of laboratory animals in ophthalmology and vision studies.

Nine weeks after grouping, rats were anesthetized by intraperitoneal injection of 3% pentobarbital sodium (30 mg/kg). The left eyeball of all rats were detected by a color Doppler ultrasound to obtain retinal hemodynamic indexes and central artery hemorheology indexes and then the blood sample and retinal tissue or the whole eyeballs were collected for the subsequent experiments followed by cervical dislocation for euthanasia. The death of rats was determined by no respiration.

Grouping and disposing

Sixty successfully modeled rats were randomly selected and divided into 6 groups with 10 rats in each group and the rest were euthanatized by cervical dislocation under narcotism by intraperitoneal injection of 3% pentobarbital sodium (30 mg/kg). There were 7 groups in this study: control group (healthy rats), model group (diabetes rats injected with normal saline via caudal vein), NC (negative control) agomir group (diabetes rats injected with NC mimic via caudal vein), miR-874 agomir group (diabetes rats injected with miR-874 mimic via caudal vein), miR-874 anti-agomir group (diabetes rats injected with miR-874 inhibitor via caudal vein), EVP4593 group (diabetes rats injected with EVP4593 via caudal vein), and miR-874 anti-agomir + EVP4593 group (diabetes rats injected with miR-874 inhibitor and EVP4593). The details of grouping were shown in Table 1. EVP4593 was NF-κB signaling pathway antagonist. The above agentia at a concentration of 4.5 nM were injected into rats at the dose of 80 mg/kg via caudal vein, once every three days for 4 weeks [20]. Eight weeks later, rats were fasted for 8 h. Then blood was drawn via caudal vein to measure blood glucose by the One Touch II glucometer (USA). Rats were weighed. The experimental design was shown in Fig. 1.

Retinal hemodynamic indexes and central artery hemorheology indexes detection in diabetes rats

Nine weeks after grouping, the rat eyeball was examined by a color Doppler ultrasound, and hemodynamic indexes of the left eye such as end-diastolic velocity (EDV), peak systolic velocity (PSV) and central retinal vein (CRV) were detected in all rats. After the rats were fasted for 20 h, rats were anesthetized by intraperitoneal injection of 3% pentobarbital sodium (30 mg/kg) and then anticoagulated

blood was drawn via the abdominal aorta. Plasma viscosity (PV), blood viscosity (BV) and erythrocyte sedimentation rate (ESR) at different shear rates were measured with a blood viscometer. The experiment was performed in triplicate.

Detection of number of retinal vascular endothelial cells and pericytes

The eyeballs of all rats were fixed. Retinal vascular digest preparations were performed. Number of retinal vascular endothelial cells (VEC) and capillary pericytes (IPC) was counted by using a microscope. All experiment was performed in triplicate.

Separation of retinal tissue

The eyeballs of rats were extirpated under aseptic conditions. The bulbar conjunction was removed. The cornea was separated at 1 mm from the posterior of corneoscleral limbus followed by the evisceration of crystalline lens and the removal of vitreous body under a stereomicroscope. The retina was isolated along the underpart of the retina, and the optic nerve was cut off. The retina was dissociated and cut into pieces.

qRT-PCR (Real-time fluorescence quantitative polymerase chain reaction)

Total RNA in the retinal tissue was extracted by the Trizol method (Invitrogen, Calsbad, CA, USA). After purity determination, the RNA was reversely transcribed into cDNA according to the instruction of TaqMan MicroRNA Assays Reverse Transcription primer (4427975, Applied Biosystems, USA) with reaction conditions of 37 °C for 30 min and 85 °C for 5 s. Primers were synthesized by the Wuhan Branch of Sangon Biotech (Shanghai) Co., Ltd., China and the sequences were listed in Table 2. Reaction condition of qRT-PCR was: pre-denaturation at 95 °C for 10 min followed by 40 circles of denaturation at 95 °C for 10 s, annealing at 60 °C for 20 s and extending at 72 °C for 34 s. Reaction system of qRT-PCR was: 10 μl SYBR Premix Ex Taq^{TM} II, 0.8 μl PCR forward primer (10 μM), 0.8 μl PCR reverse primer (10 μM), 0.4 μl ROX Reference Dye II, 2.0 μl cDNA templates, and 6.0 μl sterilized distilled water. U6 was used as the internal reference of miR-195, and GAPDH was the internal reference of CD40, RORyt, Foxp3, interleukin (IL) -17, IL-10, tumor necrosis factor (TNF)-α, IL-23 and IL-8. The reaction was performed on an ABI7500 quantitative PCR amplifier (7500, ABI, USA). $2^{-\Delta\Delta Ct}$ showed the relative expression of target gene. The experiment was performed in triplicate.

Western blotting

RIPA (Beyotime Biotechnology Co., Ltd., China) was mixed with protease inhibitor and PMSF to lyse cells on the ice for 30 min. Protein concentration was measured by using BCA protein assay kit (Beijing Dingguo Changsheng Biotechnology Co., Ltd., China). Protein was separated by SDS-PAGE for 2 h and transferred to PVDF membranes. The membrane was sealed with 5% milk for 2 h and incubated at 4 °C with the addition of primary antibodies including rabbit anti-human angiopoietin2 (Ang2) (1:2,500, ab155106, Abcam, USA), p65 (1:2,500, ab32536, Abcam, USA), vascular endothelial growth factor (VEGF) (1:2,500, ab1316, Abcam, USA) and GAPDH (1:2,500, ab9485, Abcam, USA). After the membrane was washed with tris buffered saline tween (TBST) three times, horse radish peroxidase-labeled IgG (1:10,000, ab6721, Abcam, USA) was added and incubated at room temperature for 1 h. Then the membrane was washed with TBST three times. Color development was carried out by electrogenerated chemiluminescence solutions. Relative expression of protein = gray value of target protein band / gray value of GAPDH band. The experiment was performed in triplicate.

Statistical analysis

Data analysis was performed by SPSS 11.5 software. The measurement data were expressed as mean ± standard deviation. Comparison among groups was performed by one-way ANOVA and post-hoc LSD-t test. $P < 0.05$ indicates that the difference is statistically significant.

Results

miR-874 targets regulating the expression of p65

The bioinformatics website predicted that there was the binding site between miR-874 and Rela (p65) (Fig. 2A), which was verified by the dual-luciferase reporter system assay. The results showed that there was no significant difference in luciferase activity between pmirGLO-Rela mut+NC mimic and pmirGLO-Rela mut+ miR-874 mimic, however, pmirGLO-Rela wt + miR-874 mimic group had significantly reduced luciferase activity than the pmirGLO-Rela mut+ miR-874 mimic group (Fig. 2B), indicating the target regulation of miR-874 on p65.

p65 expression in the retina of diabetes rats affected by miR-874

miR-874 expression in the retina was detected by qRT-PCR and Rela (p65) protein expression was measured by Western blot (Fig. 3). Compared with the control group, miR-874 expression significantly decreased, and p65 expression significantly increased in the retina in the model group. miR-874 agomir group and EVP4593 group had increased the miR-874 expression and inhibited the p65 expression, while the miR-874 anti-agomir group had opposite effects. EVP4593 could reversed the promotion effect of miR-874 anti-agomir on p65 expression. It suggested that miR-874 inhibited the NF-κB signaling pathway by suppressing p65 in DR of diabetes rats.

Symptoms and retinal injury relief of STZ-induced diabetes rats using miR-874

After modeling and treatment, blood glucose level significantly higher in the model group that that in the control group (4 mmol/l). miR-874 agomir and EVP4593 treatment slowed the soaring increase of blood glucose model mice, but miR-874 anti-agomir exacerbated it. EVP4593 neutralized the effect of miR-874 anti-agomir on modeled rats' blood glucose (Fig. 4A).

Rat weight in the control group was in regular growth. Compared with the control group, rat weight in the model group was significantly lower. miR-874 agomir and EVP4593 treatment improved the rat weight increase and the miR-874 anti-agomir group inhibited it. EVP4593 improved weight loss caused by the miR-874 anti-agomir in diabetes rats (Fig. 4B).

The abnormal expression of Ang2 and VEGF could cause retinal vascular endothelial cell damage and pro-inflammatory response. Thus, the protein expressions of VEGF and Ang2 were detected by Western Blotting (Fig. 4C and D). VEGF and Ang2 expressions significantly increased in the retina of model group ($P < 0.05$), indicating that pathological changes appeared in the retina. VEGF and Ang2 protein expressions were inhibited in the miR-874 agomir group and EVP4593 group and promoted in the miR-874 anti-agomir group. EVP4593 neutralized the promotion of miR-874 anti-agomir on VEGF and Ang2 protein expressions.

Retinopathy relief of diabetes rats using miR-874

Hemodynamic indexes of rats with DR were measured to detect retinal blood perfusion and blood supply (Fig. 5). Compared with the control group, EDV, PSV and CRV values in the model group decreased in varying degrees, indicating that insufficient retinal blood perfusion and blood supply occurred in diabetes rats. Diabetes rats with miR-874 agomir and EVP4593 treatment had increased EDV, PSV and CRV values, while the miR-874 anti-agomir group had opposite effects. EVP4593 neutralized the inhibition effect of miR-874 anti-agomir on EDV, PSV and CRV values (all $P < 0.05$). It manifested that miR-874 had an influence on hemodynamic indexes of rats with DR, and miR-874 could alleviate retinopathy of diabetes rats.

Hemorheology indexes of rats with DR were also cmeasured to further verify the alleviation of miR-874 on DR (Fig. 6). Compared with the control group, BV, PV and ESR increased in the model group. Diabetes rats with miR-874 agomir and EVP4593 treatment had decreased BV, PV and ESR values, while the miR-874 anti-agomir group had opposite effects. EVP4593 neutralized the promotion effect of miR-874 anti-agomir on BV, PV and ESR at all shear rates (all $P < 0.05$). It demonstrated that miR-874 relieved retinopathy of diabetes rats.

Number of retinal capillary VEC and IPC was detected (Fig. 7). Compared with the control group, number of IPC significantly reduced, and number of VEC significantly increased in the retinal capillary in the model group. Diabetes rats with miR-874 agomir and EVP4593 treatment had increased number of IPC and decreased VEC proliferation in the retinal capillary, while the miR-874 anti-agomir group had opposite effects. EVP4593 partly reversed the IPC number decrease and VEC proliferation increase caused by miR-874 anti-agomir (all $P < 0.05$). It showed that miR-874 relieved retinopathy of diabetes rats.

Discussion

Diabetes is a prevalent disease that occurs all around the world. Neuropathy, microangiopathy and macroangiopathy are main pathological features of diabetes complications. Among them, DR is the most common one, which is caused by retinal vascular leakage, inflammatory response and neovascularization. DR is also the leading cause of blindness in working-age population. The main treatment methods for DR are laser photocoagulation treatment, hyperbaric oxygen therapy and drug therapy [21]. However, these methods may lead to severe adverse side effects, such as visual acuity decrease, contrast sensitivity decrease and visual field damage. Therefore, the more efficient therapeutic strategies are needed to be developed for DR patients.

NF-κB is a nuclear transcription factor and participates in the generation process of multiple cytokines [22, 23]. It mainly plays a role in biological processes, such as biological immunity and inflammation. NF-κB includes five members: RelB, RelA (also known as p65), c-Rel, p100/p52 and p105/p50. p65-50 is the most widespread and most important NF-κB heterodimer [24-26]. The retina experiences many metabolic disorders, and changes appear in gene expressions. The progression of diabetes can result in retinal capillary cell death and histopathological changes. NF-κB was activated in the retina of diabetes, and the activated NF-κB increased capillary cell apoptosis [27], which was anterior to the development of histopathological features of DR [28]. Once NF-κB was activated in the pathogenesis of early DR, its function could only be inhibited partially by early reconstruction. Moreover, if the hyperglycemia induced by diabetes was not well controlled for 7 months, it could be irreversible. In this study, there were heightened EDV, PSV of central retinal artery (CRA) and blood velocity of CRV, lowered PV, BV and ESR at all shear rates, increased number of retinal capillary pericytes, decreased endothelial cell proliferation, and significantly reduced p65 expression in the retina in the EVP4593 group as compared to the model group. It indicated that the inhibition of NF-κB signaling pathway significantly improved the condition of DR in rats, which was consistent with the results in the literature we reviewed.

Recently, miRNA has been identified as a biomarker for the diagnosis of various diseases including DR. Moreover, there are growing evidences that miRNAs play a key role in regulating NF-κB activation and its downstream function. However, the mechanism of miRNA on NF-κB activation or inhibition in DR has not been fully revealed. miR-874 plays a role in various diseases, including several types of cancers, such as colorectal cancer, gastric cancer and non-small cell lung cancer [29]. miR-874 is significantly down-regulated in sertoli cells of diabetes rats and miR-874 overexpression relieves the renal injury of diabetes rats [30]. However, there is no study on the relationship between miR-874 and DR.

In this study, by bioinformatics prediction we found a targeted site where miR-874 bound to p65 which was the most important protein in the NF-κB signaling pathway. Moreover, dual-luciferase reporter system assay confirmed that p65 was the target gene of miR-874. DR model rats was successfully established to explore the relationship between miR-874 and NF-κB signaling pathway. The results showed that miR-874 mimic has similar therapeutic effects with NF-κB signaling pathway antagonist EVP4593 in DR rats. DR was aggravated after the treatment of miR-874 inhibitor for diabetes rats. EVP4593 counteracted the aggravation of retinopathy that was caused by miR-874 inhibitor. These results indicated that miR-874 up-regulation inhibited the expression of NF-κB signaling pathway, alleviating retinopathy in diabetes rats.

In addition, we found that the blood glucose level in the miR-874 agomir group and EVP4593 group was the lowest in model rats. In this study, diabetes rats were first established and then treated. Moreover, compared with the miR-874 agomir group and EVP4593 group, the NF-κB signaling pathway of diabetes rats in other groups was not inhibited or only partially inhibited, and correspondingly their retinopathy was more severe. Therefore, the amelioration effect of miR-874 on diabetic retinopathy was due not to the low blood glucose in rats, but to the fact that miR-874 inhibited the abnormal high expression of NF-κB signaling pathway (the NF-kB impairment) in the retina of diabetes rats. The signaling pathways in the body are complicated, so it remains to be seen whether the decrease of blood glucose is related to the inhibition of NF-κB signaling pathway.

In this study, the effect of miR-874 on retinopathy in diabetes rats has been confirmed, while the specific molecular mechanism between miR-874 and NF-κB is not clear. Moreover, whether overexpressed miR-874 mimic can be applied in clinical treatment still needs more experimental verification.

Conclusions

miR-874 can inhibit p65, an important protein in the NF-κB signaling pathway, in the retina of diabetes rats and further inhibit NF-κB signal, playing an alleviation effect on retinopathy. miR-874 may be a new targeted drug for the improvement of DR.

Abbreviations

DR: diabetic retinopathy; miRNA: microRNA; STZ: Streptozotocin; NC: negative control; EDV: end-diastolic velocity; PSV: peak systolic velocity; CRV: central retinal vein; PV: plasma viscosity; BV: blood viscosity; ESR: erythrocyte sedimentation rate; VEC: vascular endothelial cells; IPC: capillary pericytes; qRT-PCR: real-time fluorescence quantitative polymerase chain reaction; IL: interleukin; TNF: tumor necrosis factor; Ang2: angiopoietin2; VEGF: vascular endothelial growth factor; TBST: tris buffered saline tween; CRA: central retinal artery

Declarations

Ethical approval and consent to participate

The protocol and procedures employed were performed, ethically reviewed and approved by the Ethics Committee of Xiaogan Central Hospital (2017010) and in compliance with the statement of Association for Research in Vision and Ophthalmology for the care and use of laboratory animals in ophthalmology and vision studies.

Consent for publication

Not applicable.

Availability of data and materials

The datasets used and/or analyzed during the current study are available from the corresponding author on reasonable request.

Competing interests

The authors declare that they have no competing interests.

Funding

Not applicable.

Authors' contributions

RL contributed to conception and design and drafted the article. HMY and TZ designed the study and revised the article for important intellectual content. YMY and ZCL analyzed and interpreted of data and drafted the article. JYC and CLQ acquired the data and drafted the article. CJL contributed to conception and design and revised the article for important intellectual content. All authors have read and approved the manuscript.

Acknowledgments

Not applicable.

References

1. Brinchmann-Hansen O, Dahl-Jorgensen K, Hanssen KF, Sandvik L. The response of diabetic retinopathy to 41 months of multiple insulin injections, insulin pumps, and conventional insulin therapy. Archives of ophthalmology (Chicago, Ill : 1960). 1988;106(9):1242-6.
2. Xie MY, Yang Y, Liu P, Luo Y, Tang SB. 5-aza-2'-deoxycytidine in the regulation of antioxidant enzymes in retinal endothelial cells and rat diabetic retina. International journal of ophthalmology. 2019;12(1):1-7.
3. Obeid A, Su D, Patel SN, Uhr JH, Borkar D, Gao X, et al. Outcomes of Eyes Lost to Follow-up with Proliferative Diabetic Retinopathy That Received Panretinal Photocoagulation versus Intravitreal Anti-Vascular Endothelial Growth Factor. Ophthalmology. 2019;126(3):407-13.
4. Joussen AM, Poulaki V, Mitsiades N, Kirchhof B, Koizumi K, Dohmen S, et al. Nonsteroidal anti-inflammatory drugs prevent early diabetic retinopathy via TNF-alpha suppression. FASEB journal : official publication of the Federation of American Societies for Experimental Biology. 2002;16(3):438-40.
5. Zheng L, Szabo C, Kern TS. Poly(ADP-ribose) polymerase is involved in the development of diabetic retinopathy via regulation of nuclear factor-kappaB. Diabetes. 2004;53(11):2960-7.
6. Kamble VV, Kokate RD . Automatic Identification and Classification of Microaneurysms, Exudates and Blood Vessel for Early Diabetic Retinopathy Recognition: Computational Intelligence in Data Mining. 2019.
7. Hemanth DJ DO, Kose U. An enhanced diabetic retinopathy detection and classification approach using deep convolutional neural network. Neural Computing and Applications. 2019(7398):1-15.
8. Thomas AA, Biswas S, Feng B, Chen S, Gonder J, Chakrabarti S. lncRNA H19 prevents endothelial-mesenchymal transition in diabetic retinopathy. Diabetologia. 2019;62(3):517-30.
9. Luo DW, Zheng Z, Wang H, Fan Y, Chen F, Sun Y, et al. UPP mediated Diabetic Retinopathy via ROS/PARP and NF-kappaB inflammatory factor pathways. Current molecular medicine. 2015;15(8):790-9.
10. Chen F, Zhang HQ, Zhu J, Liu KY, Cheng H, Li GL, et al. Puerarin enhances superoxide dismutase activity and inhibits RAGE and VEGF expression in retinas of STZ-induced early diabetic rats. Asian Pacific journal of tropical medicine. 2012;5(11):891-6.
11. Yin Y, Chen F, Wang W, Wang H, Zhang X. Resolvin D1 inhibits inflammatory response in STZ-induced diabetic retinopathy rats: Possible involvement of NLRP3 inflammasome and NF-kappaB signaling pathway. Molecular vision. 2017;23:242-50.
12. Liang Z, Gao KP, Wang YX, Liu ZC, Tian L, Yang XZ, et al. RNA sequencing identified specific circulating miRNA biomarkers for early detection of diabetes retinopathy. American journal of physiology Endocrinology and metabolism. 2018;315(3):E374-e85.

13. Zhang J, Wu L, Chen J, Lin S, Cai D, Chen C, et al. Downregulation of MicroRNA 29a/b exacerbated diabetic retinopathy by impairing the function of Muller cells via Forkhead box protein O4. Diabetes & vascular disease research. 2018;15(3):214-22.
14. Wang W, Lo ACY. Diabetic Retinopathy: Pathophysiology and Treatments. International journal of molecular sciences. 2018;19(6).
15. Sorrentino FS, Matteini S, Bonifazzi C, Sebastiani A, Parmeggiani F. Diabetic retinopathy and endothelin system: microangiopathy versus endothelial dysfunction. Eye (London, England). 2018;32(7):1157-63.
16. Meerson A, Eliraz Y, Yehuda H, Knight B, Crundwell M, Ferguson D, et al. Obesity impacts the regulation of miR-10b and its targets in primary breast tumors. BMC cancer. 2019;19(1):86.
17. Chen PJ, Shang AQ, Yang JP, Wang WW. microRNA-874 inhibition targeting STAT3 protects the heart from ischemia-reperfusion injury by attenuating cardiomyocyte apoptosis in a mouse model. Journal of cellular physiology. 2019;234(5):6182-93.
18. Yao T, Zha D, Gao P, Shui H, Wu X. MiR-874 alleviates renal injury and inflammatory response in diabetic nephropathy through targeting toll-like receptor-4. Journal of cellular physiology. 2018;234(1):871-9.
19. Gong Q, Li F, Xie J, Su G. Upregulated VEGF and Robo4 correlate with the reduction of miR-15a in the development of diabetic retinopathy. Endocrine. 2019.
20. Wang G, Yan Y, Xu N, Hui Y, Yin D. Upregulation of microRNA-424 relieved diabetic nephropathy by targeting Rictor through mTOR Complex2/Protein Kinase B signaling. Journal of cellular physiology. 2019;234(7):11646-53.
21. Berteau F, Rouviere B, Nau A, Le Berre R, Sarrabay G, Touitou I, et al. 'A20 haploinsufficiency (HA20): clinical phenotypes and disease course of patients with a newly recognised NF-kB-mediated autoinflammatory disease'. Annals of the rheumatic diseases. 2019;78(5):e35.
22. Aeschlimann FA, Laxer RM. Response to: 'A20 haploinsufficiency (HA20): clinical phenotypes and disease course of patients with a newly recognised NF-kB-mediated autoinflammatory disease' by Aeschlimann et al. Annals of the rheumatic diseases. 2019;78(5):e36.
23. Huang WJ, Wang Y, Liu S, Yang J, Guo SX, Wang L, et al. Retraction notice to "Silencing circular RNA hsa_circ_0000977 suppresses pancreatic ductal adenocarcinoma progression by stimulating miR-874-3p and inhibiting PLK1 expression" [Cancer Letters 422C (2018) 70-80]. Cancer letters. 2018;438:232.
24. Tang W, Wang W, Zhao Y, Zhao Z. MicroRNA-874 inhibits cell proliferation and invasion by targeting cyclin-dependent kinase 9 in osteosarcoma. Oncology letters. 2018;15(5):7649-54.
25. Liao H, Pan Y, Pan Y, Shen J, Qi Q, Zhong L, et al. MicroRNA874 is downregulated in cervical cancer and inhibits cancer progression by directly targeting ETS1. Oncology reports. 2018;40(4):2389-98.
26. Zhang Y, Wang X, Zhao Y. MicroRNA874 prohibits the proliferation and invasion of retinoblastoma cells by directly targeting metadherin. Molecular medicine reports. 2018;18(3):3099-105.

27. Antzelevitch C. Genetic, molecular and cellular mechanisms underlying the J wave syndromes. Cardiac Electrophysiology: from Cell to Bedside. 2018;76(5):483-93.
28. Jiang T, Guan LY, Ye YS, Liu HY, Li R. MiR-874 inhibits metastasis and epithelial-mesenchymal transition in hepatocellular carcinoma by targeting SOX12. American journal of cancer research. 2017;7(6):1310-21.
29. Yang R, Li P, Zhang G, Lu C, Wang H, Zhao G. Long Non-Coding RNA XLOC_008466 Functions as an Oncogene in Human Non-Small Cell Lung Cancer by Targeting miR-874. Cellular physiology and biochemistry : international journal of experimental cellular physiology, biochemistry, and pharmacology. 2017;42(1):126-36.
30. Leong KW, Cheng CW, Wong CM, Ng IO, Kwong YL, Tse E. miR-874-3p is down-regulated in hepatocellular carcinoma and negatively regulates PIN1 expression. Oncotarget. 2017;8(7):11343-55.

Tables

Table 1 Grouping methods of rats

Group	Rat type	Treatment
Control	Healthy control rats	Injection of the same amount of normal saline via caudal vein
Model	Diabetes model rats	Model rats (Streptozotocin-treated model rats)
Negative control agomir	Diabetes model rats	Streptozotocin + overexpressed negative control vector
miR-874 agomir	Diabetes model rats	Streptozotocin + miR-874 mimic
miR-874 anti-agomir	Diabetes model rats	Streptozotocin + miR-874 inhibitor
EVP4593	Diabetes model rats	Streptozotocin + NF-κB signaling pathway antagonist EVP4593
miR-874 anti-agomir + EVP4593	Diabetes model rats	Streptozotocin + miR-874 inhibitor + EVP4593

Table 2 Primer sequence

Gene	Primer sequence (5’-3’)
miR-874	Forward: GGGCGGCCCCACGCACCA
	Reverse: GTGCAGGGTCCGAGGT
U6	Forward: CTCGCTTCGGCAGCACA
	Reverse: AACGCTTCACGAATTTGCGT

Figures

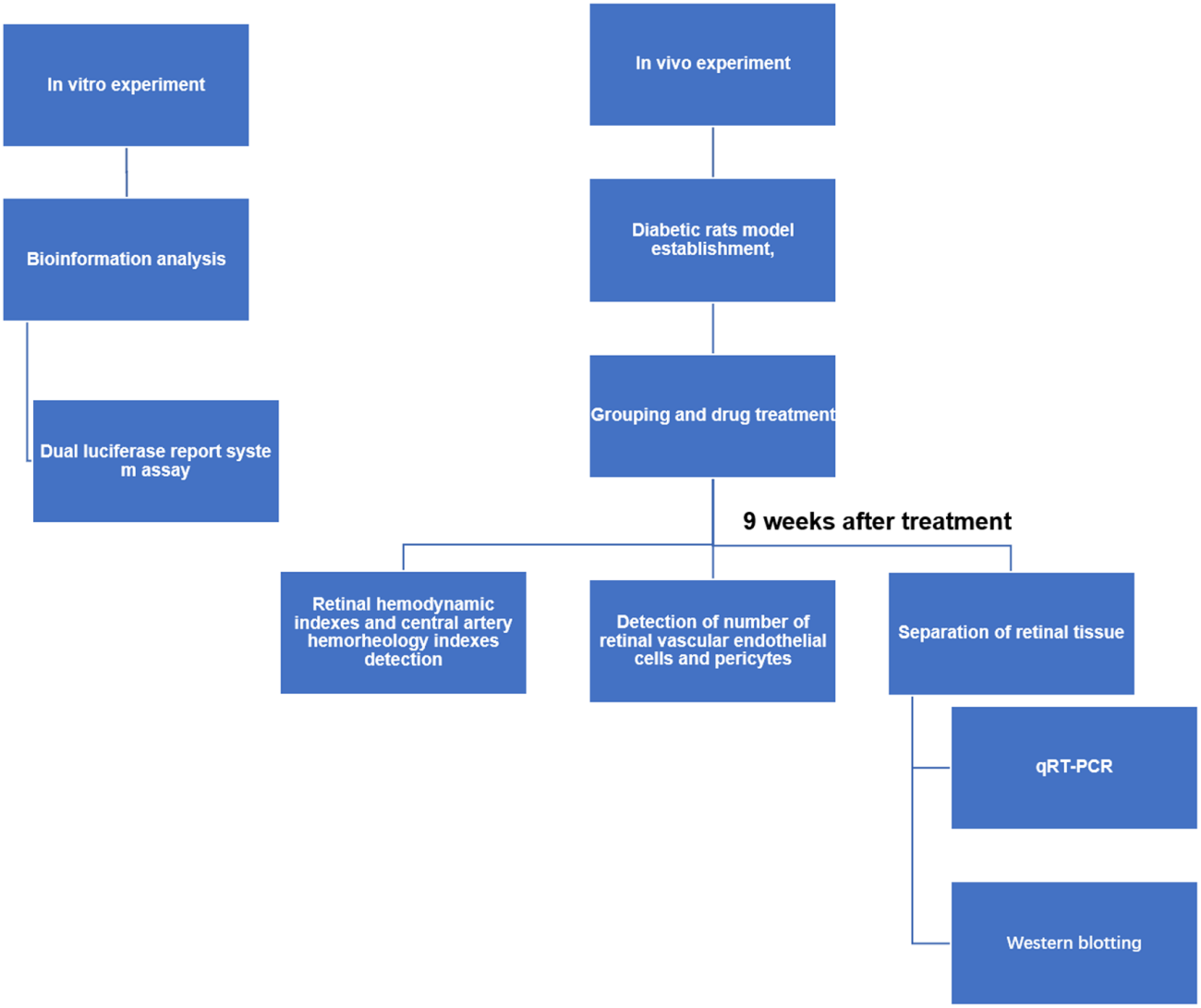

Figure 1

Experimental design flow diagram. qRT-PCR real-time fluorescence quantitative polymerase chain reaction

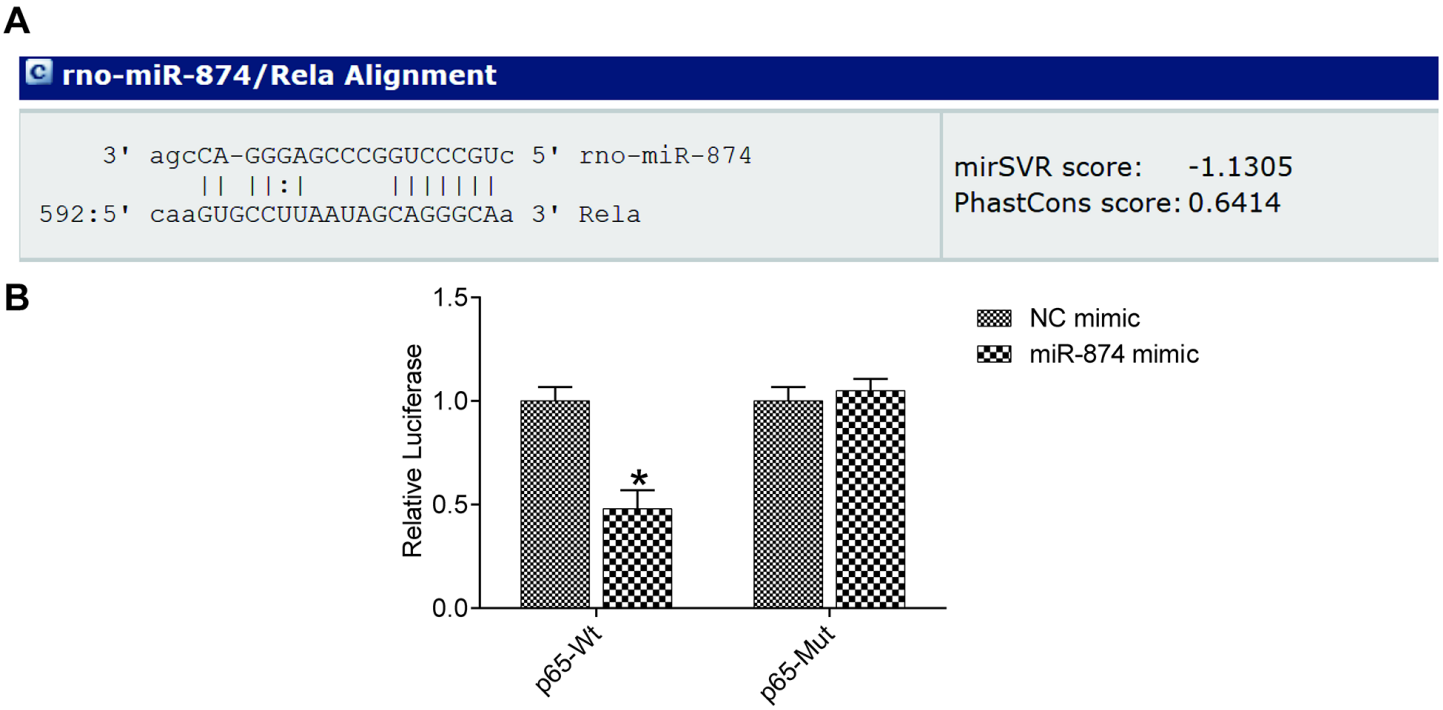

Figure 2

Bioinformatics prediction and dual-luciferase reporter assay results. A: There was the binding site between miR-874 and p65 that predicted by a bioinformatics website; B: Dual-luciferase reporter system assay verified the target relationship between miR-874 and p65 in HEK 293T cell line. The experiment was independently repeated three times. Compared with the NC mimic group, *P < 0.05. NC negative control; Wt wild type; Mut mutant

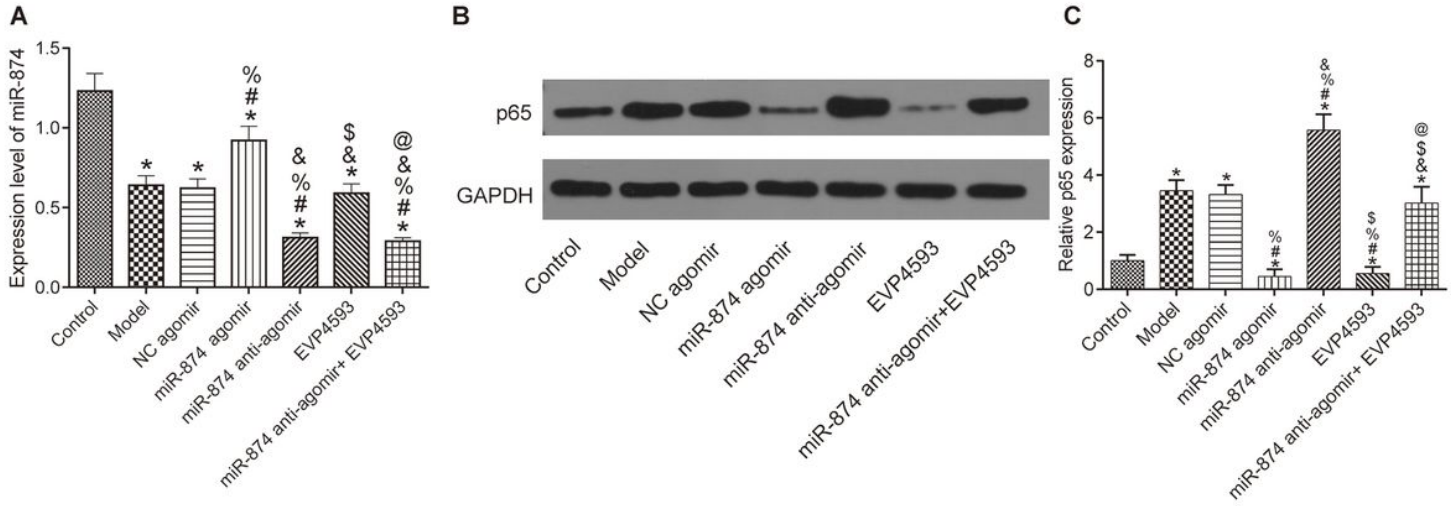

Figure 3

miR-874 and P65 expressions in the retina. A: miR-874 expression; B: Protein bands; C: Protein expression. Compared with the control group, *P < 0.05; compared with the model group, #P < 0.05; compared with the NC agomir group, %P < 0.05; compared with the miR-874 agomir group, &P < 0.05; compared with the miR-874 anti-agomir group, $P < 0.05; compared with the EVP4593 group, @P < 0.05. NC negative control

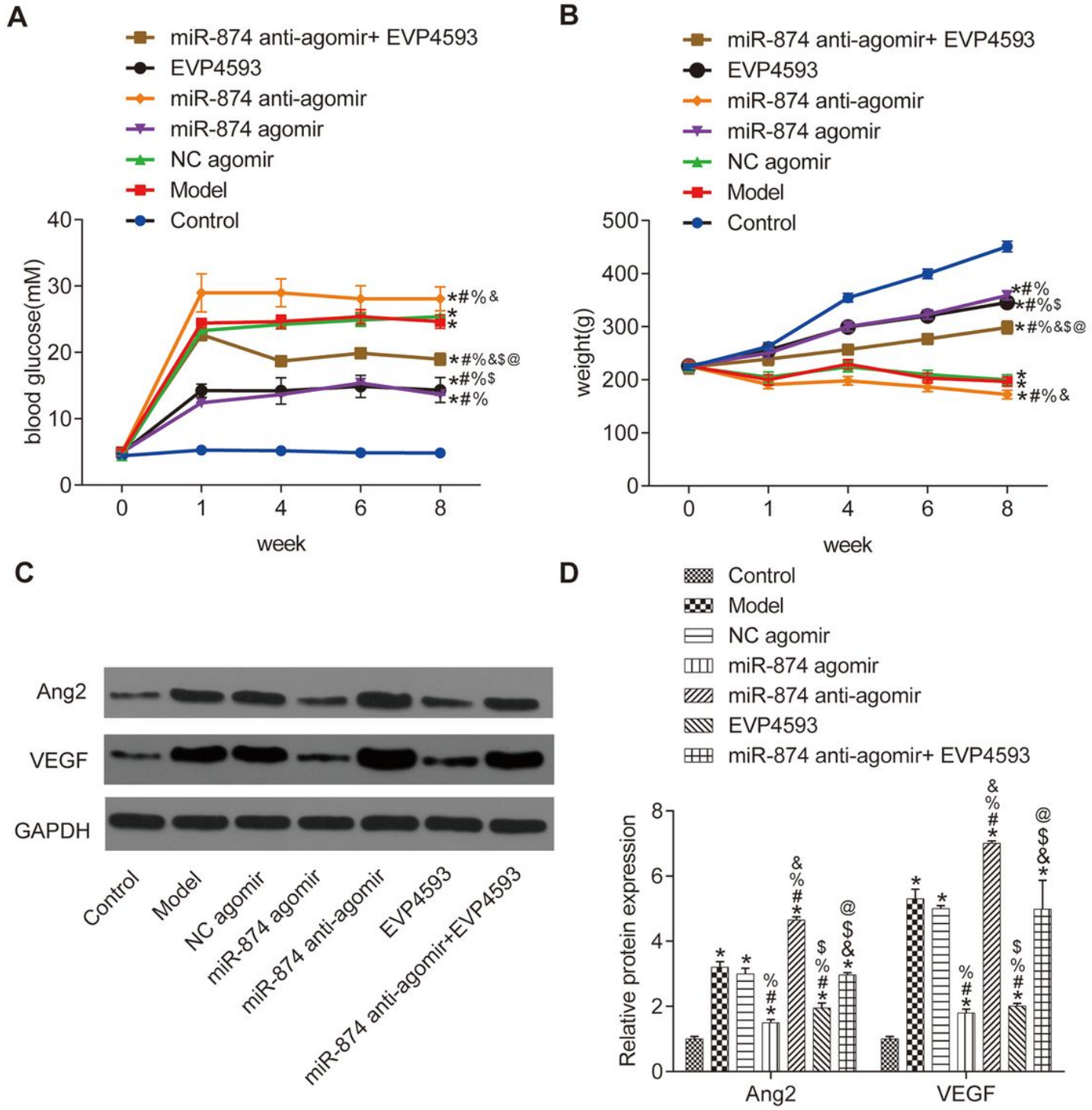

Figure 4

Retinal pathological changes detection. A: Blood glucose; B: Weight; C: Protein bands of Ang2 and VEGF in the retina of STZ-induced diabetes rat models; D: Protein expression histogram. Compared with the control group, *P < 0.05; compared with the model group, #P < 0.05; compared with the NC agomir group, %P < 0.05; compared with the miR-874 agomir group, &P < 0.05; compared with the miR-874 anti-agomir group, $P < 0.05; compared with the EVP4593 group, @P < 0.05. NC negative control; VEGF vascular endothelial growth factor; Ang2 angiopoietin2; STZ streptozotocin

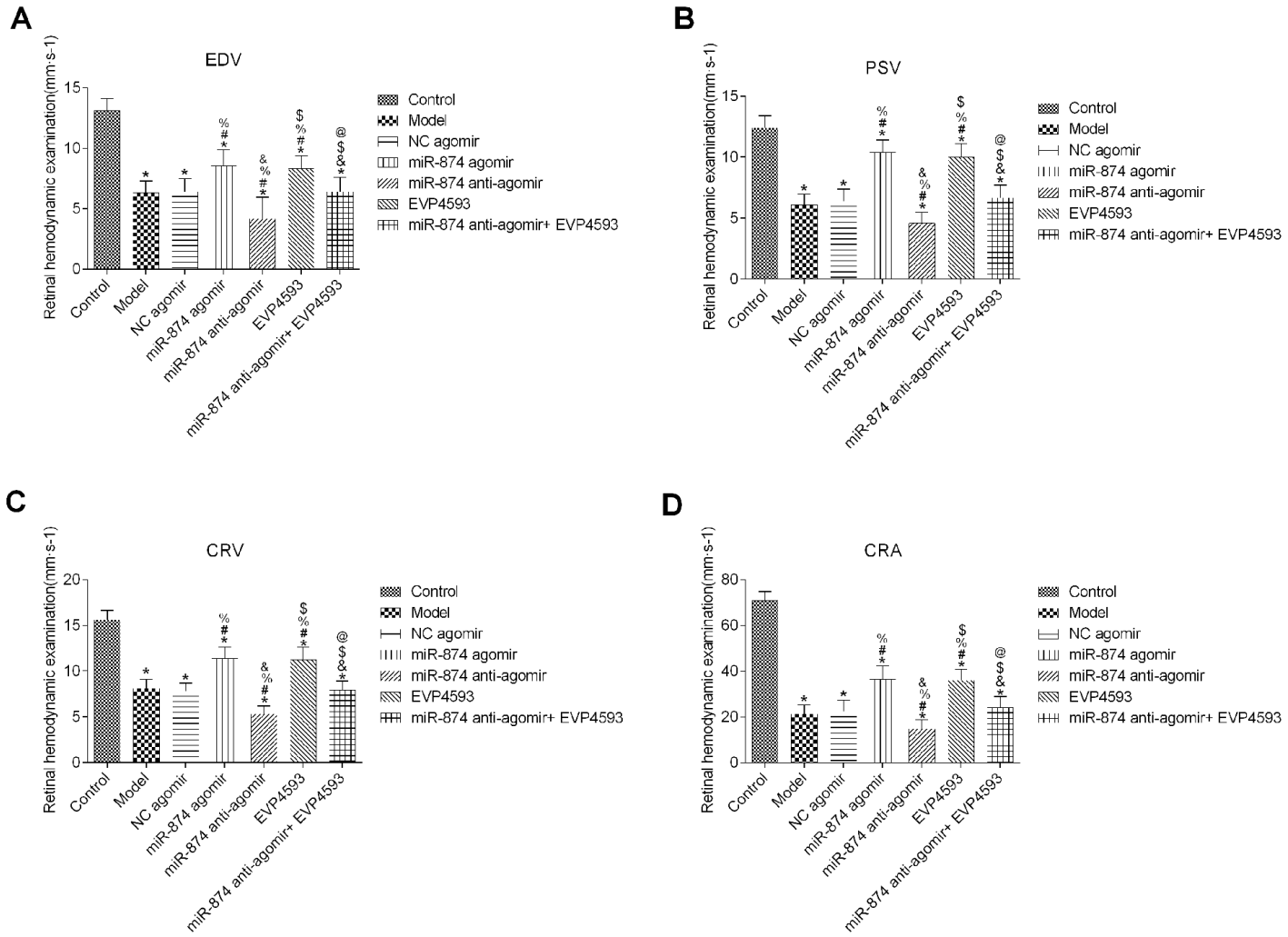

Figure 5

Retinal hemodynamic examinations of diabetes rats. A: End-diastolic velocity; B: Peak systolic velocity of central retinal artery; C: Blood velocity of central retinal vein; D: Blood velocity of central retinal artery. Compared with the control group, *P < 0.05; compared with the model group, #P < 0.05; compared with the NC agomir group, %P < 0.05; compared with the miR-874 agomir group, &P < 0.05; compared with the miR-874 anti-agomir group, $P < 0.05; compared with the EVP4593 group, @P < 0.05. NC negative control; EDV end-diastolic velocity; PSV peak systolic velocity; CRV central retinal vein; CRA central retinal artery

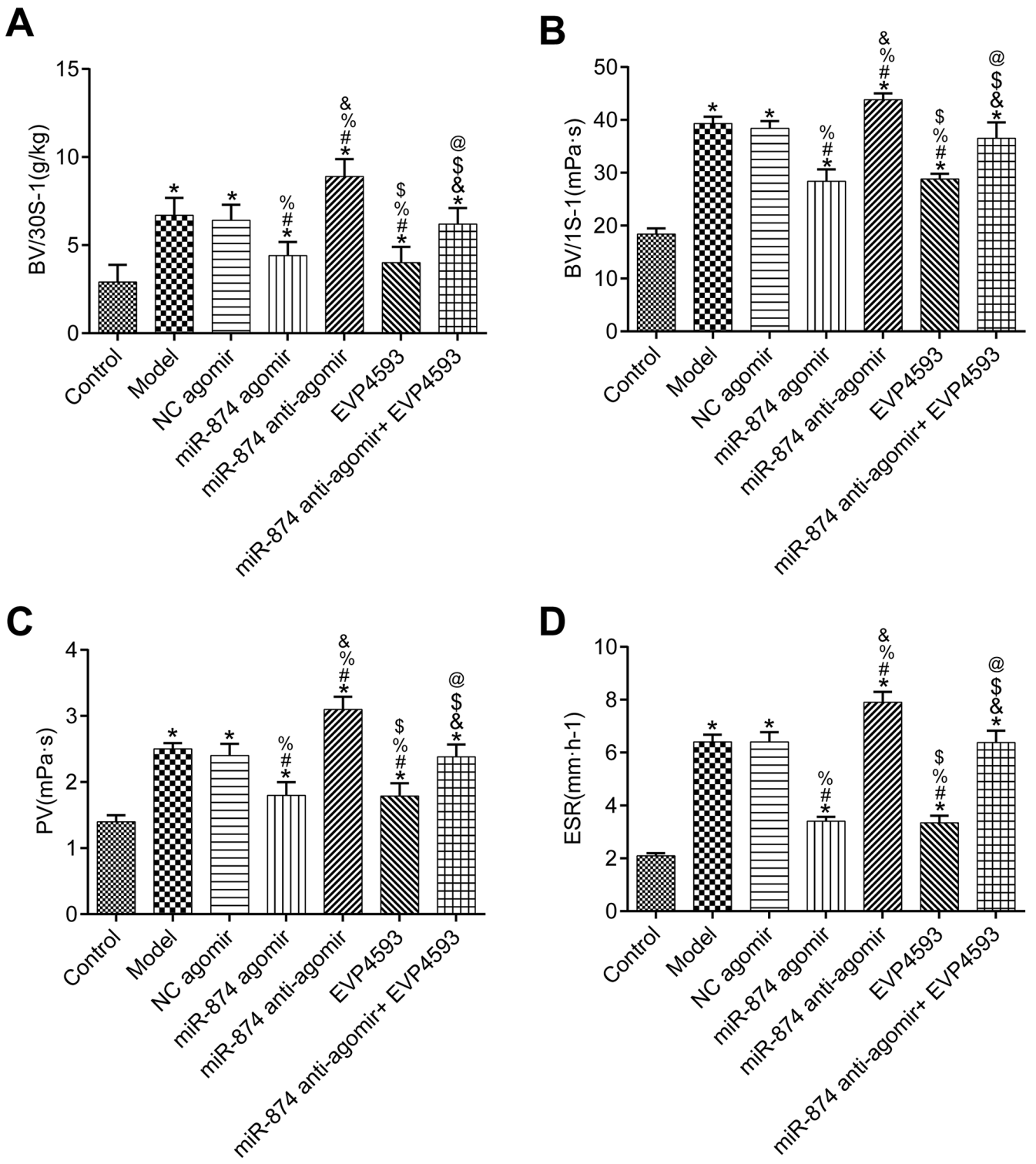

Figure 6

Retinal hemorheology of diabetes rats. A: BV/30S-1; B: BV/1S-1; C: PV; D: ESR. Compared with the control group, *P < 0.05; compared with the model group, #P < 0.05; compared with the NC agomir group, %P < 0.05; compared with the miR-874 agomir group, &P < 0.05; compared with the miR-874 anti-agomir group, $P < 0.05; compared with the EVP4593 group, @P < 0.05. NC negative control; BV blood viscosity; PV plasma viscosity; ESR erythrocyte sedimentation rate

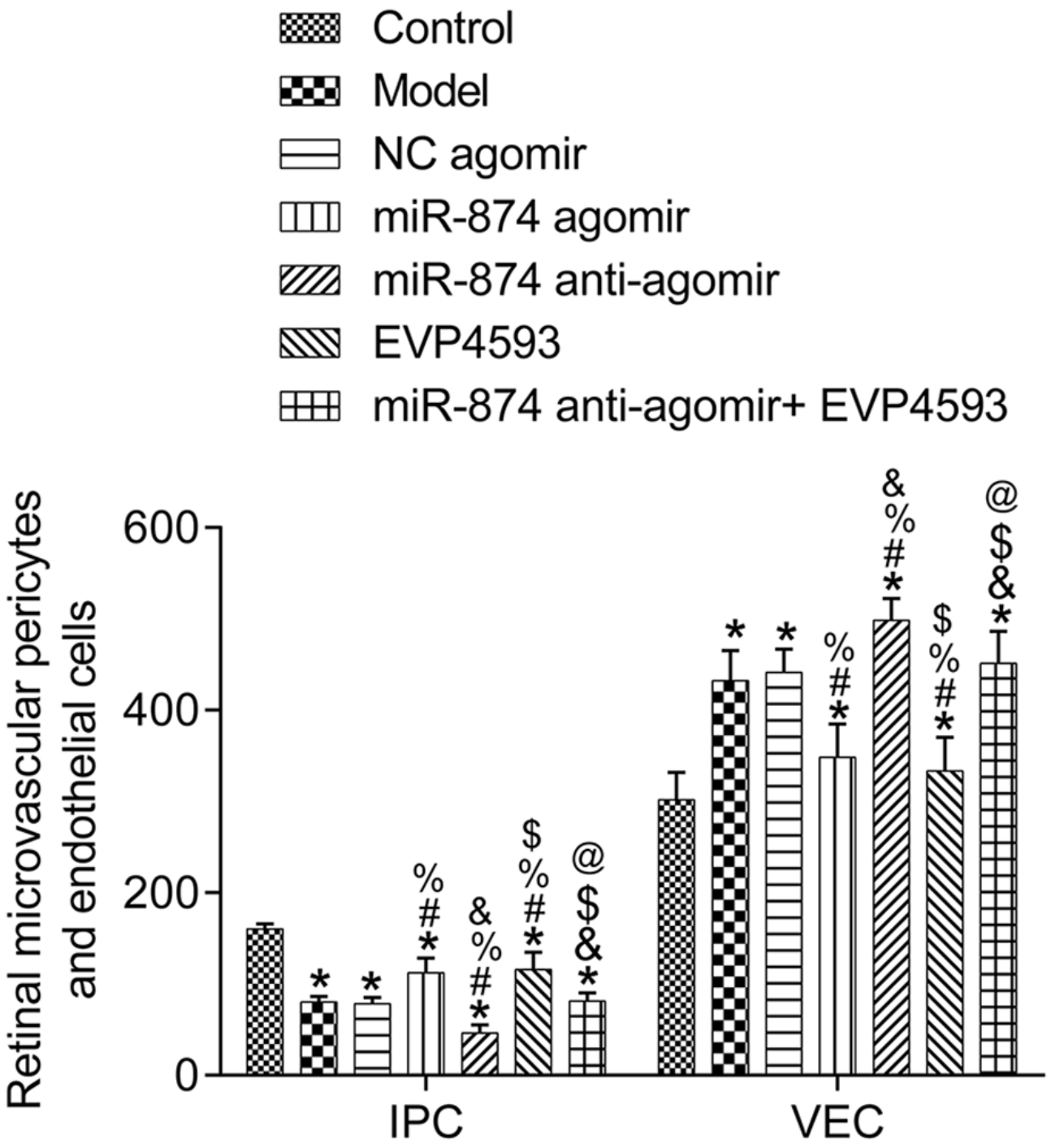

Figure 7

Number of retinal microvascular pericytes and endothelial cells. Compared with the control group, *P < 0.05; compared with the model group, #P < 0.05; compared with the NC agomir group, %P < 0.05; compared with the miR-874 agomir group, &P < 0.05; compared with the miR-874 anti-agomir group, $P < 0.05; compared with the EVP4593 group, @P < 0.05. NC negative control; IPC pericytes; VEC endothelial cells

Supplementary Files

This is a list of supplementary files associated with this preprint. Click to download.

- NC3RsARRIVEGuidelinesChecklistfillable.pdf